A Case Study on a Quasi-Stationary Meiyu Front Bringing About Continuous Rainstorms with Piecewise Potential Vorticity Inversion*

ZHAO Yuchun[1,2†](赵玉春), LI Zechun[3](李泽椿), and XIAO Ziniu[3](肖子牛)

1 *Wuhan Institute of Heavy Rain of CMA, Wuhan* 430074
2 *Wuhan Central Meteorological Observatory, Wuhan* 430074
3 *National Meteorological Center, Beijing* 100081

(Received December 18, 2007)

ABSTRACT

A 4-day persistent rainstorm resulting in serious flooding disasters occurred in the north of Fujian Province under the influences of a quasi-stationary Meiyu front during 5–8 June 2006. With $1° \times 1°$ latitude and longitude NCEP reanalysis data and the ground surface rainfall, using the potential vorticity (PV) analysis and PV inversion method, the evolution of main synoptic systems, and the corresponding PV and PV perturbation (or PV anomalies) and their relationship with heavy rainfall along the Meiyu front are analyzed in order to investigate the physical mechanism of the formation, development, and maintenance of the Meiyu front. Furthermore, the PV perturbations related to different physics are separated to investigate their different roles in the formation and development of the Meiyu front. The results show: the formation and persistence of the Meiyu front in a quasi-WE orientation are mainly due to the maintenance of the high-pressure systems in its south/north sides (the West Pacific subtropical high/ the high pressure band extending from the Korean Peninsula to east of North China). The Meiyu front is closely associated with the PV in the lower troposphere. The location of the positive PV perturbation on the Meiyu front matches well with the main heavy rainfall area along the Meiyu front. The PV inversion reveals that the balanced winds satisfying the nonlinear balanced assumption represent to a large extent the real atmospheric flow and its evolution basically reflects the variation of stream flow associated with the Meiyu front. The unbalanced flow forms the convergence band of the Meiyu front and it mainly comes from the high-pressure system in the north side of the Meiyu front. The positive PV perturbation related to latent heat release in the middle-lower troposphere is one of the main factors influencing the formation and development of the Meiyu front. The positive vorticity band from the total balanced winds is in accordance with the Meiyu front band and the magnitude of the positive vorticity from the balanced wind is very close to that from real winds. The PV perturbation in the boundary layer is to a certain degree favorable for the formation and development of Meiyu front. In general, the lower boundary potential temperature perturbation is not beneficial to the formation and development, which is attributed to the relatively low surface temperature due to surface evaporation and solar short-wave radiation reduction shaded by clouds on the Meiyu front band, however, it has some diurnal variation. The effect of PV perturbation in the upper troposphere on the formation and development of the Meiuyu front is relatively weaker than others' and not beneficial to the formation and development of the Meiyu front, but it is enhanced in the period of Meiyu front's fast southward movement when the deep North China trough develops and moves southeastward. Rest PV perturbation unrelated to latent heat release in the middle-lower troposphere plays a certain role in the Meiyu front's fast southward movement. Lastly, it should be pointed out that the different PV perturbations maybe play a different role in different stages of the Meiyu front development.

Key words: Meiyu front, rainstorm, PV (potential vorticity) inversion, diabatic heating

1. Introduction

In early summer of every year, a long Meiyu frontal band usually maintains from southern China to the south of Japan. Its formation and maintenance often bring abundant rainfall and exert an important influence on the weather in East Asia. The nature and structure of Meiyu front are different from the

*Supported by Heavy Rain Opening Fund IHR2007K4 of IHR, CMA.
†Corresponding author: zhaoych@cma.gov.cn.

mid-latitude polar front, with rather weak horizontal temperature gradient but strong cyclonic shear in the two sides of the front (Kato and Martin, 1985). Chen and Chang (1980) pointed out that the Meiyu front has different structures in the west and east part. The east part is of baroclinic characteristics and has strong temperature gradient, tilting vertically to the upper-air cold center. The west part is of tropical features. Liu et al. (2003) and Chen and Gao (2006) made a further analysis and numerical study on the Meiyu front structure. Recently, Zhao et al. (2004) claimed that the Meiyu front was of multi-scale features, and advanced a multi-scale conceptual model and researched the mechanism of mesoscale convective system formation and development. Wang and Li (2002), Wang et al. (2003), and Jiang and Ni (2005) carried out the diagnostic analysis and numerical simulation on the mesoscale convective system along the Meiyu front. Wu et al. (2004) systematically investigated the frontogenesis of Meiyu front and external forcing factors influencing Meiyu frontogenesis. Cho and Chen (1995) put forward a hypothesis of interaction between low-level potential vorticity and cumulus convection. However, there have been few documents pointing out the role of different physics in the formation and maintenance of the Meiyu front and their relative importance.

Potential vorticity (PV) is a useful diagnostic variable, which is conservative and invertible under the adiabatic and frictionless condition. In the 1980s, Hoskins et al. (1985) pointed out that the adiabatic and frictionless atmosphere tends to move on a two-dimensional isentropic surface and the PV is of plentiful dynamics. Given a PV, balanced condition, and boundary condition, the height and wind fields can be induced. They also thought that the isentropic PV is a useful tool to study atmospheric dynamics. Later, Davis (1992) advanced an inversion method of separated perturbation PV, i.e., the PV anomaly generated by non-conservative processes is separated with PV's conservative feature, the effects of different PV on the wind and pressure fields can be diagnosed by perturbed PV inversion method, and the physical causes for some phenomena can be deduced. After that, the PV inversion method has been widely applied in the atmospheric researches. For example, Hakim et al. (1996) studied the interaction of upper-level PV anomaly related to upper-level south and north trough with the background flows using the quasi-geostrophic PV inversion, and found that the background flows determined the interaction between vortices. Huo et al. (1999) found that the two upper-air short waves played an important role in the determination of tropospheric flow structure related to superstorm with Eterl PV inversion. Wu et al. (2004) diagnosed the main factors affecting typhoon. Furthermore, Huo et al. (1998) tried to assimilate the surface observational information into the numerical model initial field to improve the numerical forecast with PV inversion method, and viewed it as a potential tool. Demirtas and Thorpe (1999) modified the local PV to improve short-range numerical weather prediction with satellite vapor images. Recently, Chen et al. (2003) carried out an investigation of Meiyu front in early summer with PV inversion and hypothesized that the CISK associated with diabatic processes is the mechanism of the formation and maintenance of the Meiyu front and the low-level jet. Zhou et al. (1998) made a diagnostic analysis of the abrupt outburst cyclone in western Pacific with PV inversion. In addition, other related analysis and research with the PV inversion method was rare.

A west-east oriented quasi-stationary Meiyu front formed on 4 June 2006. During 5–7 June, it was pushed southward to the south of the Yangtze River and the north of South China, and maintained stationary over there. On 8 June, the west part of the Meiyu front was pushed southward quickly while the east part was motionless and affected most parts of Fujian Province. During this period, mesoscale convective systems formed and developed un-intermittently on the Meiyu front and brought about heavy rains of several-days in the north of Fujian Province, which induced serious flooding disasters over there and led to severe economic losses and some fatalities. Here, this long-time maintained Meiyu frontal heavy rain is taken as an example to analyze in detail the main synoptic patterns and the relationship of the Meiyu front evolution with the lower tropospheric PV during the period of the Meiyu front's formation, development, and movement. Meanwhile, the PV perturbations related to different physics are separated and inversed with Eterl PV inversion method to investigate the role and contribution of different PV perturbations in the Meiyu front and reveal the physical mechanism of Meiyu front's formation and development.

2. Synoptic case descriptions

2.1 The formation of the Meiyu front

A quasi-WE-oriented rain band formed at 2000 BT 3 June 2006. This indicates that the Meiyu front begins to form (Fig.1a). At this time, a dense band of pseudo-equivalent potential temperature ($\theta_{\rm se}$) contour (Meiyu front) at 850 hPa was in a quasi-WE orientation in the south of the Yangtze River, extending eastward from the north of Guizhou Province to the south of Zhejiang Province, across Hunan Province and the north of Jiangxi Province. There were several important weather systems in the middle-lower troposphere: the low-level West Pacific subtropical high, the high pressure band extending westward from the Korean Peninsula to the east of North China, and a low

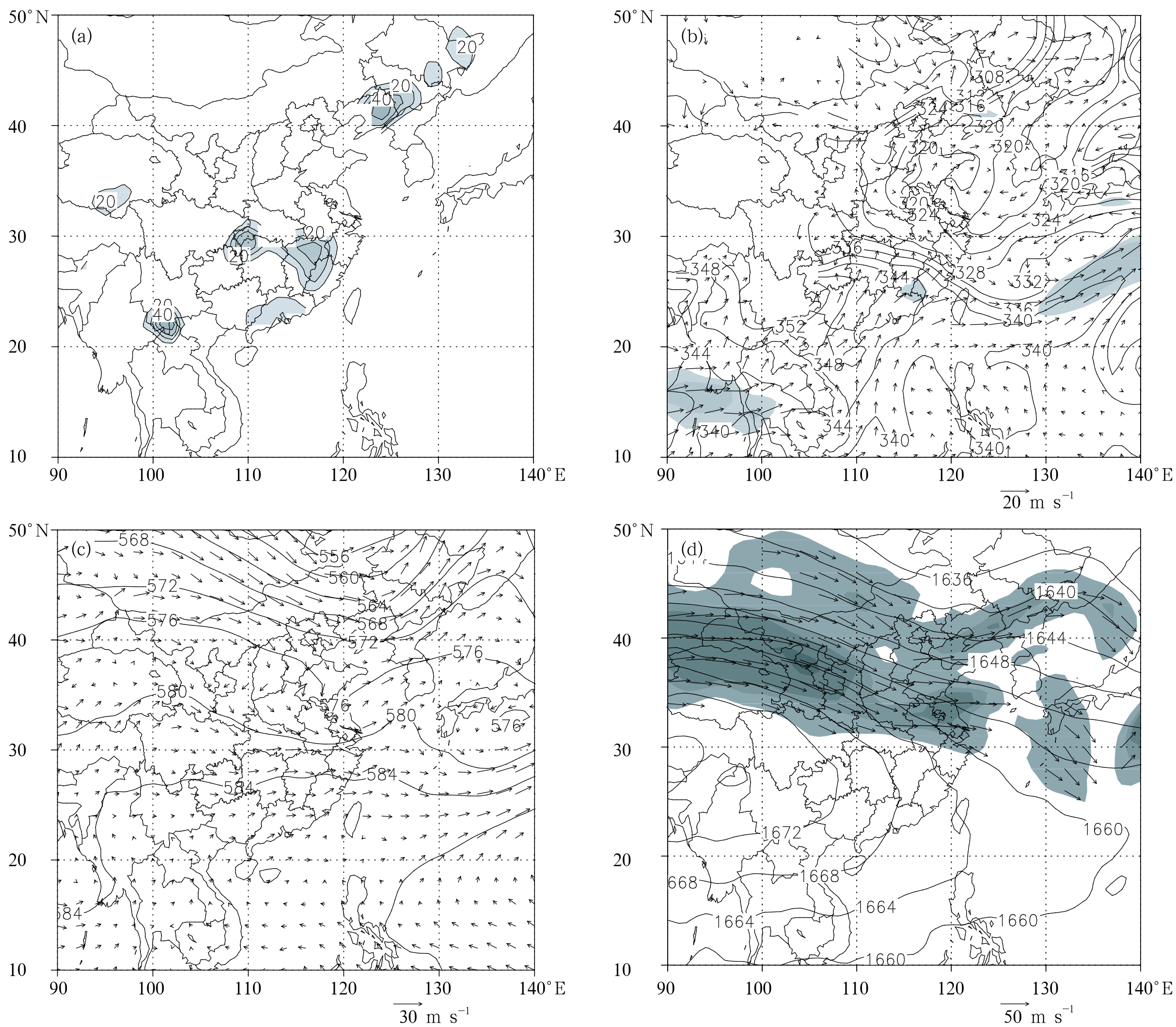

Fig.1. (a) Observed 6-h accumulative precipitation (mm), (b) 850-hPa wind field (shading: $\geqslant$12 m s^{-1}) and pseudo-equivalent potential temperature (solid line; K), (c) 500-hPa geopotential height (dagpm) and wind fields, and (d) 100-hPa geopetential height (solid line; dagpm) and 200-hPa upper-level jet stream (vectors; shading: $\geqslant$30 m s^{-1}) at 2000 BT 3 June 2006.

pressure band between them, with the Meiyu front in it. The height field was in a "high-low-high" pattern. Viewed from the streamline at 850 hPa, there was a positive vorticity band along the Meiyu front, with southwest winds and east winds in its two sides. The low-level jet was not established totally in the south of Meiyu front, but 12-m s^{-1} wind velocity disturbance occured on the large wind axis (Fig.1b). At 500 hPa, the main body of the West Pacific subtropical high was to the east of 125°E, with a flat west flow over the Meiyu front and a shallow low trough in North China (Fig.1c). At 100 hPa, the east part of the South Asian high ridge was in a WN-SE direction, with diffluent northwest and northeast winds over the Meiyu front and the upper level of the strong rainfall area (the north of Jiangxi Province) on the Meiyu front happening to be a strong divergence area. At 200 hPa, the upper-level jet stream axis was in a WN-SE orientation and to the north of Meiyu front, with jet stream core on the jet stream axis, and the heavy rainfall in the north of Jiangxi Province being in the right side of the jet stream core entrance (Fig.1d).

2.2 The development and maintenance of the Meiyu front

Due to the large-scale circulation being stable, the "high-low-high" circulation from the south to the north at 850-hPa height field maintained continuously and did not change obviously. At 0800 BT 5 June, the Meiyu front rain band was located in the south of the Yangtze River and the north of South China, but the strong heavy rain shifted eastward to the north of Fujian Province (Fig.2a). The circulation pattern in the mid-lower level of troposphere started to change, with a closed high pressure anti-cyclonic circulation forming in the east of North China at 850 hPa. The prevailing east winds at the bottom of high pressure were to the north of Meiyu front, with southwest or west winds in the south of Meiyu front. The quasi-WE oriented Meiyu front extended eastward from 105° to 125°E. The low-level jet to the south of the front was intensified with its size increased (Fig.2b). At 500 hPa, the West Pacific subtropical high began to extend westward to 115°E, with its ridge line near 16°N. A high pressure ridge started to develop in the north of Xinjiang Region and it was strengthened step by step and moved eastward. The northwest flow in front of the ridge steered the North China high to the sea (Fig.2c). At 100 hPa, the distribution of the South Asian high was not obviously changed. The upper-level westerly jet stream at 200 hPa further propagated eastward, with the core on the jet stream axis also propagating to the east, and the influence of upper-level jet stream on the north of Fujian Province was weakened.

2.3 The fast southward shifting of the Meiyu front

At 0200 BT 7 June, the Meiyu frontal rain band started to be in an NE-SW direction. At this time, under the steering of the northwest flow in front of the 500-hPa high pressure ridge, the high pressure in the east of North China at 850 hPa shifted to the sea. A low trough (NE-SW oriented shear line) in the northwest of North China began to push southward, with northwest winds in the behind of the trough beginning to confluence to the west of the Yangtze River. Under this circulation, the quasi-WE oriented Meiyu frontal shear line was changed, with its west part quickly pushed to the south of Hunan Province and the north of Guangxi Region under the northwest flows in the rear of the low trough in the northwest of North China. The Meiyu front started to be in an NE-SW direction, with a cold shear line between northwest and southwest winds in the two sides of the Meiyu front respectively. Due to the anti-cyclonic high pressure circulation in the east of North China moving to the sea, the east winds to the north of the Meiyu front east part changed into southeast winds (or even south winds). It was a weak warm shear between southwest and southeast winds. But the east part of Meiyu front was still maintained and influenced most parts of Fujian Province, due to the anti-cyclonic high pressure in the east of North China not obvious shifting southward in the period of its moving to the sea. At 850 hPa, the positive vorticity band was the same as Meiyu front and in an NE-SW direction. The 100-hPa South Asian high was enhanced and its ridge line began to be in a W-E orientation, with its ridge line still maintaining near 27°–28°N.

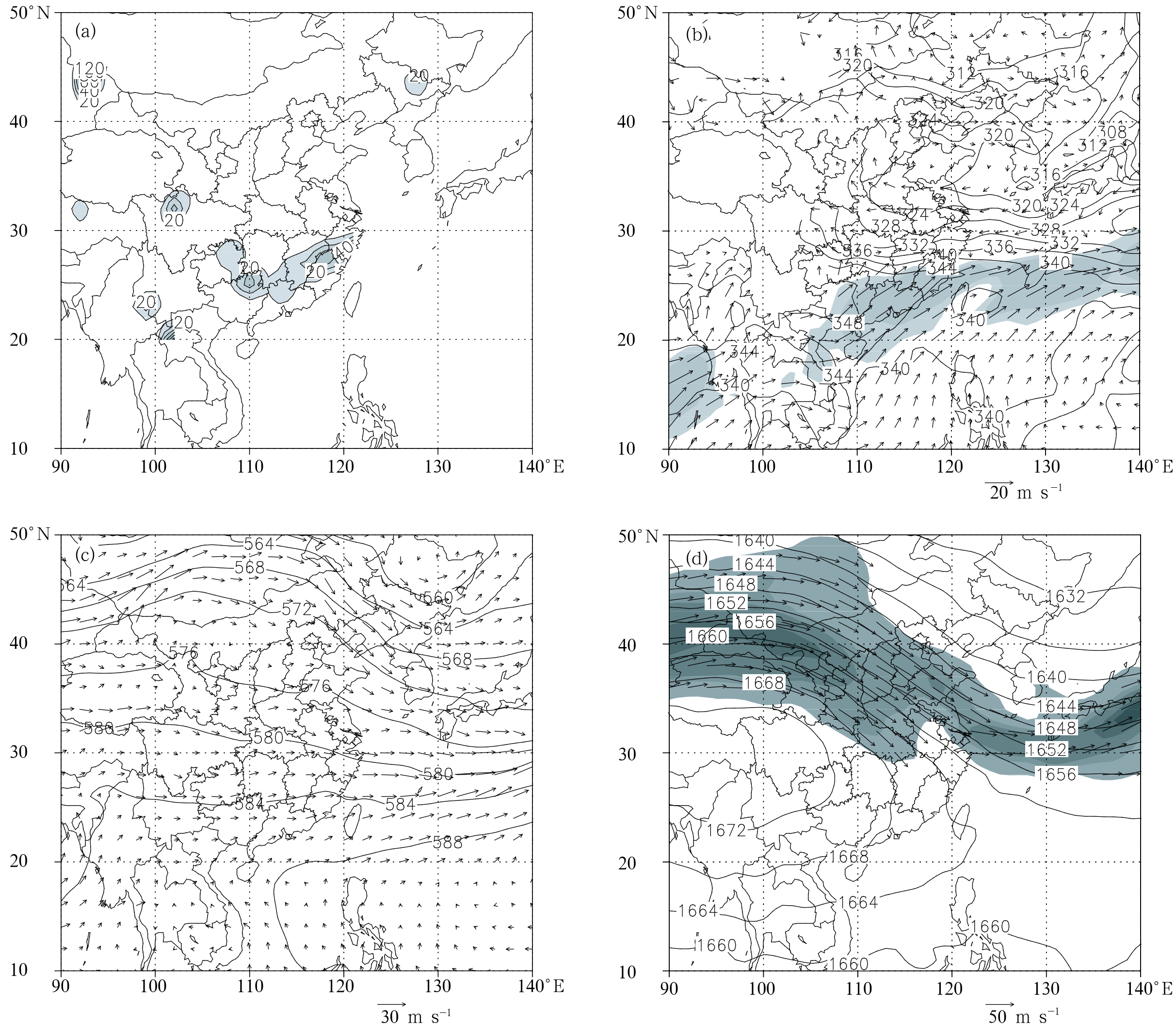

Fig.2. As in Fig.1, but for 0800 BT 5 June 2006.

2.4 The disappearance of the Meiyu frontal rain band in land

At 0800 BT 10 June, there was no obvious rainfall in the south of the Yangtze River and South China, i.e., the Meiyu frontal rain band in land disappeared. It is found, in the analysis of 850-hPa stream field and θ_{se} (figure omitted), that under the effect of the strong northwest flow in rear of North China low trough, the Meiyu front was pushed southward to south of 22°N, with the south of the Yangtze River and South China under the control of northwest flows in the rear of the Meiyu front. The dense area of θ_{se} and positive vorticity band were in an NE-SW orientation, extending northeastward from the north of the South China Sea to the south of Japanese Sea, with SW low level jet band in the south of the Meiyu front. At 500 hPa, a deep low trough was established in the coast of East Asia. Under its pushing, the West Pacific subtropical high became in an NE-SW direction. At 100 hPa, the east of South Asian high contracted and came down to the south, with 200-hPa upper-level westerly jet stream down to south of 30°N.

3. PV and PV anomalies

The Ertel potential vorticity (EPV) of baroclinic compressive fluids is

$$EPV = \frac{1}{\rho}\eta \cdot \nabla\theta, \tag{1}$$

where ρ is the air density, η is the three-dimensional absolute vorticity vector, and θ is the potential temperature. The EPV is conservative in a three-dimensional inviscid adiabatic atmosphere. Under p coordination, the EPV can be written as

$$EPV = -g \cdot [(f + \frac{\partial v}{\partial x} - \frac{\partial u}{\partial y})\frac{\partial \theta}{\partial p} + \frac{\partial u}{\partial p}\frac{\partial \theta}{\partial y} - \frac{\partial v}{\partial p}\frac{\partial \theta}{\partial x}]. \quad (2)$$

In the following, every 6-h NCEP reanalysis data are used to calculate the EPV, the average of 48 $EPVs$ during 1–12 June 2006, and the perturbed EPV (or EPV anomaly, $EPVA$) at different time. Then, it is investigated the relationship of Meiyu front with Meiyu frontal rainfall in its different stages.

In the stage of Meiyu front formation (2000 BT 3 June), a long positive vorticity band forms at 110°–140°E, with a maximum PV of 0.6 PVU. The long PV band is corresponding with the positive vorticity band, and also with the Meiyu front location and orientation. Therefore, the positive vorticity band, the PV band, and dense θ_{se} band all can indicate the Meiyu front to a certain degree. On the EPVA distribution, there are two large positive EPVA centers in the south of the Yangtze River, which are consistent with the rainfall area on the Meiyu front, with a maximum EPVA of 0.3 PVU (Fig.3a). Therefore, the large-value center of EPVA denotes well the heavy rainfall area. It is conjectured that the diabatic heating by rainfall condensation release may generate PV in the low level. In the stage of Meiyu front maintenance (0800 BT 5 June), a quasi-WE-oriented positive vorticity band is

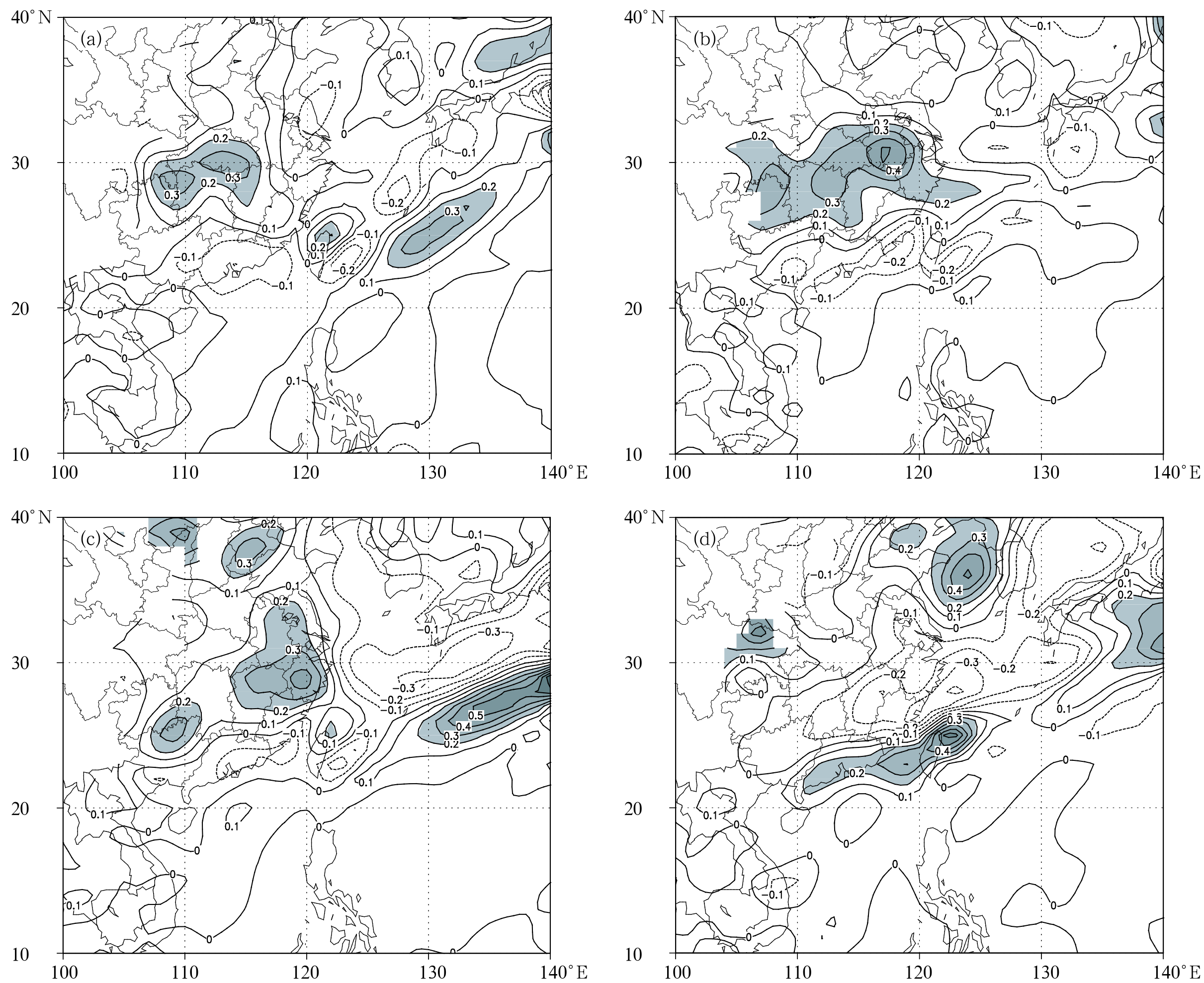

Fig.3. Distributions of 850-hPa potential vorticity perturbation (PVU) at (a) 2000 BT 3, (b) 0800 BT 5, (c) 0200 BT 7, and (d) 0800 BT 10 June 2006 (1 PVU=10^{-6} K m^2 s^{-1} kg^{-1}, shaded area: $\geqslant$0.2 PVU).

maintained from the south of the Yangtze River to South China. The maximum PV is increased and the PV in the east part of Meiyu front comes to 0.7 PVU, with rainfall intensified correspondingly. At this time, a quasi-WE-oriented positive EPVA band is consistent with the rainfall band, with a maximum EPVA of 0.5 PVU (Fig.3b). When the Meiyu front comes down to the south (0200 BT 7 June), the Meiyu front evolutes into an NE-SW oriented band and the PV band also becomes the same direction. Due to the intensified NW winds in the rear of North China low trough during the period of Meiyu front fast moving, the NE-SW oriented PV band is slightly intensified, with a maximum PV of 0.7 PVU. The EPVA band on the Meiyu front also evolves into an NE-SW band (Fig.3c), with heavy rain center still matching with the large value center of EPVA. When the Meiyu front coming down to the south of 22°N (0800 BT 10 June), the Meiyu frontal rainfall disappears in the land and the positive PV band comes to the south too. The NE-SW positive EPVA band also moves to the south of 22°N (Fig.3d).

The above analysis shows that, in the process of Meiyu front formation, development, and fast southward movement, a positive PV band always maintained and is in consistence with the direction of Meiyu front, with the heavy rainfall center matching with the large positive value center of EPVA. This implies that there exists a close relationship between the Meiyu front and the PV, and the heavy rainfall center on the Meiyu front and the large value center of EPVA. The Meiyu front can be represented by the PV. The EPVA on the Meiyu front may be related to diabatic heat feedback of Meiyu front rainfall condensation, i.e., the released diabatic heating may maintain and intensify the PV of the Meiyu front in the low level. In the following, PV inversion method is applied to research the contribution of the PV perturbations associated with different physics to the Meiyu front.

4. The PV inversion of Meiyu frontal heavy rain systems

4.1 Simple instruction of the PV inversion method

The PV is conservative and inversive under the adiabatic and frictionless condition. The inversive height and wind fields with PV inversion are balanced dynamically. Due to the stability of balanced flow evolution, the tracking and prognosis of the weather system evolution are important. On the other side, the unbalanced winds can be obtained with real winds minus balanced winds, which can be used to analyze the origin and evolution of convergence. The most important points of PV inversion lie in the fact that it can inverse separated PV perturbation relevant to different weather system or different physics, which is conducive to the understanding the role of different PV perturbation in synoptic systems and the developing mechanism of rainfall weather systems. Here, the EPV inversion is carried out with nonlinear balanced equation advanced by Charney (1962) as a balance condition to consist of a closed equation group. Under the hypothesis of non-rotational winds much less than non-divergence winds, the terms relevant to divergence and vertical velocity are neglected, and the nonlinear balanced equation under the spherical coordination can be written as

$$\nabla^2 \Phi = \nabla \cdot f \nabla \psi + \frac{2}{a^4 \cos^2\phi}\Big[\frac{\partial^2 \psi}{\partial \lambda^2}\frac{\partial^2 \psi}{\partial \phi^2} - (\frac{\partial^2 \psi}{\partial \lambda \partial \phi})^2\Big], \quad (3)$$

and the Ertel PV can be written as

$$q = \frac{g\kappa\pi}{p}\Big[(f+\nabla^2\psi)\frac{\partial^2 \Phi}{\partial \pi^2} - \frac{1}{a^2\cos^2\phi}\frac{\partial^2 \psi}{\partial \pi \partial \lambda}\frac{\partial^2 \Phi}{\partial \pi \partial \lambda} - \frac{1}{a^2}\frac{\partial^2 \psi}{\partial \pi \partial \phi}\frac{\partial^2 \Phi}{\partial \pi \partial \phi}\Big], \quad (4)$$

where Φ is the geopotential height, f is the Coliolis parameter, a is the earth's radius, ψ is the stream function of non-divergence winds, g is the gravity accelerated velocity, and p is pressure. $\kappa = R/c_{\mathrm{p}}$, $\pi = c_p(p/p_0)^\kappa$ is the Exner function ($p_0 = 10^5$ Pa). Given q and specific lateral conditions, the two variables of Φ and ψ satisfying the nonlinear balanced equation can be solved and the height, wind, and temperature fields therefore can be deduced. With small perturbation method, the above equation group is linearized. Firstly, the EPV is separated into average and perturbed field, $q(\lambda,\phi,\pi,t) = \overline{q}(\lambda,\phi,\pi) + q'(\lambda,\phi,\pi,t)$. The same is treated to Φ and ψ. Then substitute them into the equation group and neglect the nonlinear small terms. The linearized perturbation equation is obtained. Davis (1992) linearized the above equations with $[\ ]^* = [^-] + 1/2\sum_{k-1}^{K}[\ ]$. Any perturbed PV field can be divided into different parts, with the sum of their own solutions equal to the total disturbed flows (e.g., $\sum q_k = q', \sum \Phi_k = \Phi', \sum \psi_k = \psi'$). As to any perturbed q_k and its corresponding ψ_k and Φ_k, the closed PV inversion system is as follows:

$$\nabla^2 \Phi_k = \nabla \cdot (f \nabla \psi_k) + \frac{2}{a^4 \cos^2\phi} \times \Big(\frac{\partial^2 \psi^*}{\partial \lambda^2}\frac{\partial^2 \psi_k}{\partial \phi^2} + \frac{\partial^2 \psi^*}{\partial \phi^2}\frac{\partial^2 \psi_k}{\partial \lambda^2} - 2\frac{\partial^2 \psi^*}{\partial \lambda \partial \phi}\frac{\partial^2 \psi_k}{\partial \lambda \partial \phi}\Big), \tag{5}$$

$$q_k = \frac{g\kappa\pi}{p}\Big[(f + \nabla^2 \psi^*)\frac{\partial^2 \Phi_k}{\partial \pi^2} + \frac{\partial^2 \Phi^*}{\partial \pi^2}\nabla^2 \psi_k - \frac{1}{a^2\cos^2\phi}\Big(\frac{\partial^2 \psi^*}{\partial \lambda \partial \pi}\frac{\partial^2 \Phi_k}{\partial \lambda \partial \pi} + \frac{\partial^2 \Phi^*}{\partial \lambda \partial \pi}\frac{\partial^2 \psi_k}{\partial \lambda \partial \pi}\Big) - \frac{1}{a^2}\Big(\frac{\partial^2 \psi^*}{\partial \phi \partial \pi}\frac{\partial^2 \Phi_k}{\partial \phi \partial \pi} + \frac{\partial^2 \Phi^*}{\partial \phi \partial \pi}\frac{\partial^2 \psi_k}{\partial \phi \partial \pi}\Big)\Big]. \tag{6}$$

The equation is a linear system for flow perturbation ψ_k and Φ_k related to any perturbed EPV. Under the condition of $\pi = \pi_0$ and $\pi = \pi_T$, the upper and lower boundary conditions can be simply set to the Neumann boundary condition of $\partial \Phi_k/\partial \pi, \partial \psi_k/\partial \pi = -\theta_k$. Specifically, as to the total field $\partial \Phi/\partial \pi = f_0, \partial \psi/\partial \pi = -\theta$, the perturbed field can be set to $\partial \Phi_k/\partial \pi = f_0, \partial \psi_k/\partial \pi = -\theta_k$. The lateral condition can be set to the Dirichlet condition. Since the contribution of individual EPVA to the flow is unknown in advance, it is hard to determine a suitable lateral boundary condition. In calculation, a domain larger than the interested area is selected. A uniform lateral boundary condition is set as zero to every ψ_k and Φ_k. The selection of the average has a great influence on the calculation of perturbed PV. Usually, the mean is computed in a synoptic period. But due to the quasi-stationary feature of the Meiyu front, the average of height, temperature, wind, and PV is calculated in the period of 1–12 June 2006. Then the perturbation of height, temperature, wind, and PV is computed. Lastly, perturbed PV inversion is carried out to get the balanced height and wind satisfying the nonlinear balanced equation and deduce relevant temperature field.

4.2 The verifications of inversive results

Figure 4 shows 850-hPa heights and relative vorticity and corresponding inversive ones satisfying the nonlinear equation at 2000 BT 4 June 2006. The pattern of inversive height field is very similar to the analyzed, and with systematically higher height. Chen et al. (2003) pointed out that the heights are systematically higher after EPV inversion analysis, due to the fact that the inversion is constrained by the nonlinear balanced equation and only the rotational part of the flow is reserved. Thus the results are acceptable. Besides, the inversive heights are smoother and this is also an unavoidable default of EPV inversion. The relative vorticity calculated from inversive balanced winds is basically consistent with the analyzed. Though there is a negative vorticity area in the north of Meiyu front, with its size larger than the analyzed, the vorticity field deduced from inversed winds describes well the positive vorticity band associated with the Meiyu front. Therefore, the inversion results are suitable in the analysis of Meiyu front.

4.3 The evolution of the balanced flow

The flow deduced by EPV inversion is satisfying the nonlinear balanced equation. It belongs to nonlinear balanced flow and is quasi-balanced. Therefore, the analysis of the relationship between the balanced flow's evolution and Meiyu front and heavy rain is of significant importance. Figure 5 is 850-hPa EPV-inversed non-divergence winds and its relative vorticity satisfying the nonlinear balanced equation in the different stages of Meiyu front development. In Stage I, there is a weak cyclonic circulation in the north of Hunan Province, which leads to the rainfall generation there and is of importance to the west part of Meiyu front, with a corresponding positive vorticity. In the south of the Yangtze River, a strong SW flow starts to establish in the south side of Meiyu front. There is a weak meso-α-scale anti-cyclonic circulation in the Korean Peninsula, at the bottom of which no obvious east winds form. Hence, it is a weak shear between southwest and south flows in the east of Meiyu front, where there is no obvious rainfall. In Stage II, a strong anti-cyclonic circulation forms in Korea to the east of North China. The east wind at the bottom of the circulation and strong southwest flow in the south of Meiyu front constitute the Meiyu front shear line.

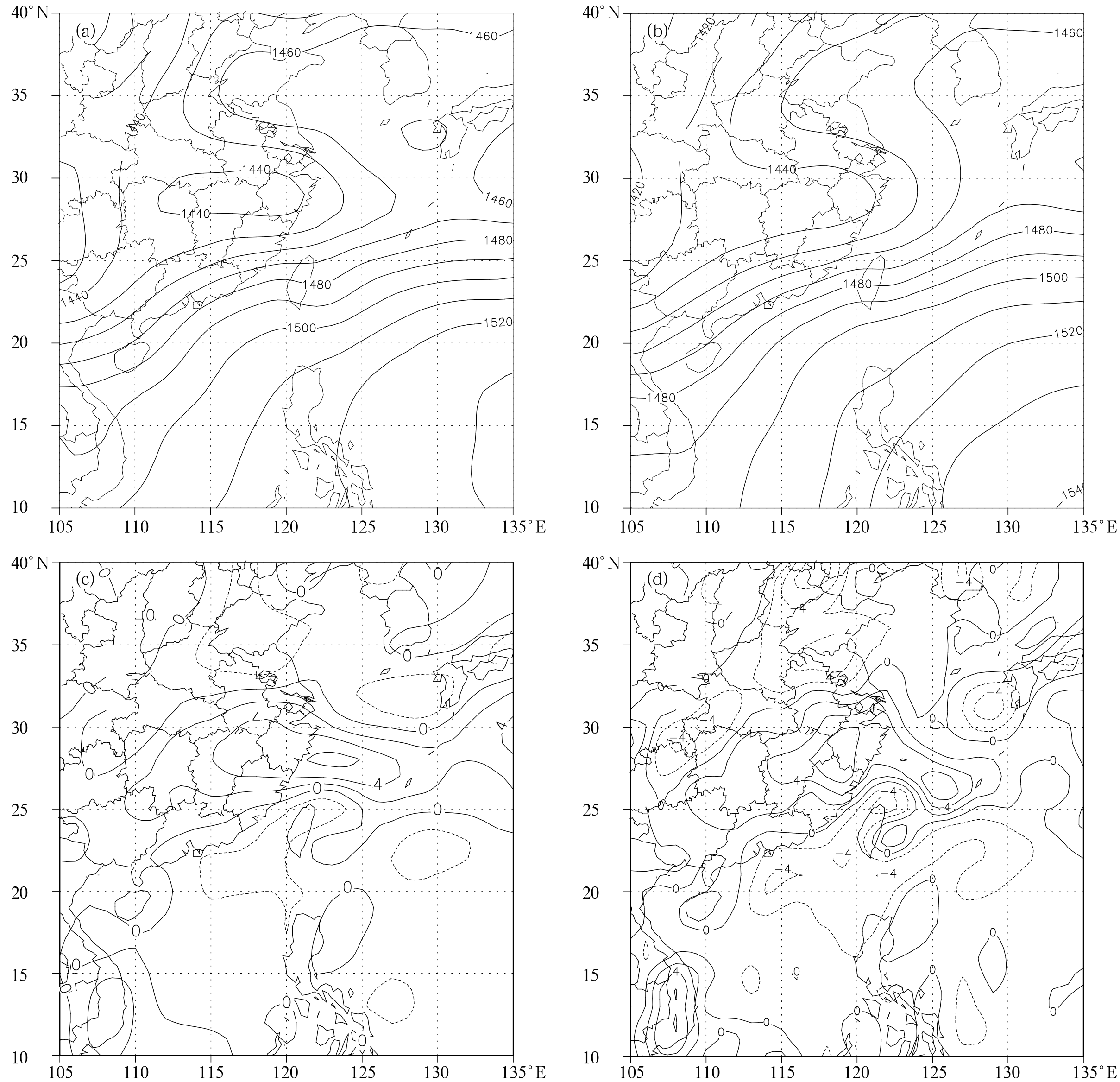

Fig.4. Distributions of (a) 850-hPa geopotential height (gpm), (c) relative vorticity (10^{-5} s^{-1}), and corresponding EPV-inversed (b) geopotential height and (d) relative vorticity satisfying the nonlinear balanced equation at 2000 BT 4 June 2006.

At the same time, the shear formed by balanced flow in the east part is stronger than that in the west. The heavy rainfall also mainly takes place in the east part. Therefore, the balanced high pressure system in the two sides of Meiyu front plays a significant role in the formation, maintenance, and development of Meiyu front, which is consistent with the analysis of Section 2. In Stage III, there exists an important steering system−a strong North China low trough (cold shear line), which pushes the Meiyu front quickly translating southward. At this time, a high-pressure anti-cyclonic circulation in the north of Meiyu front shifts east to the south of Korean Peninsula, with the low-level jet in the south of the Meiyu front also pushing southward. At 0800 BT 10 June, a new low trough forms in North China and the Meiyu front shifted to the south of 22°N.

The above analysis indicates that the EPV-inversed balanced flow satisfying the nonlinear balanced equation can represent the real flow to a large

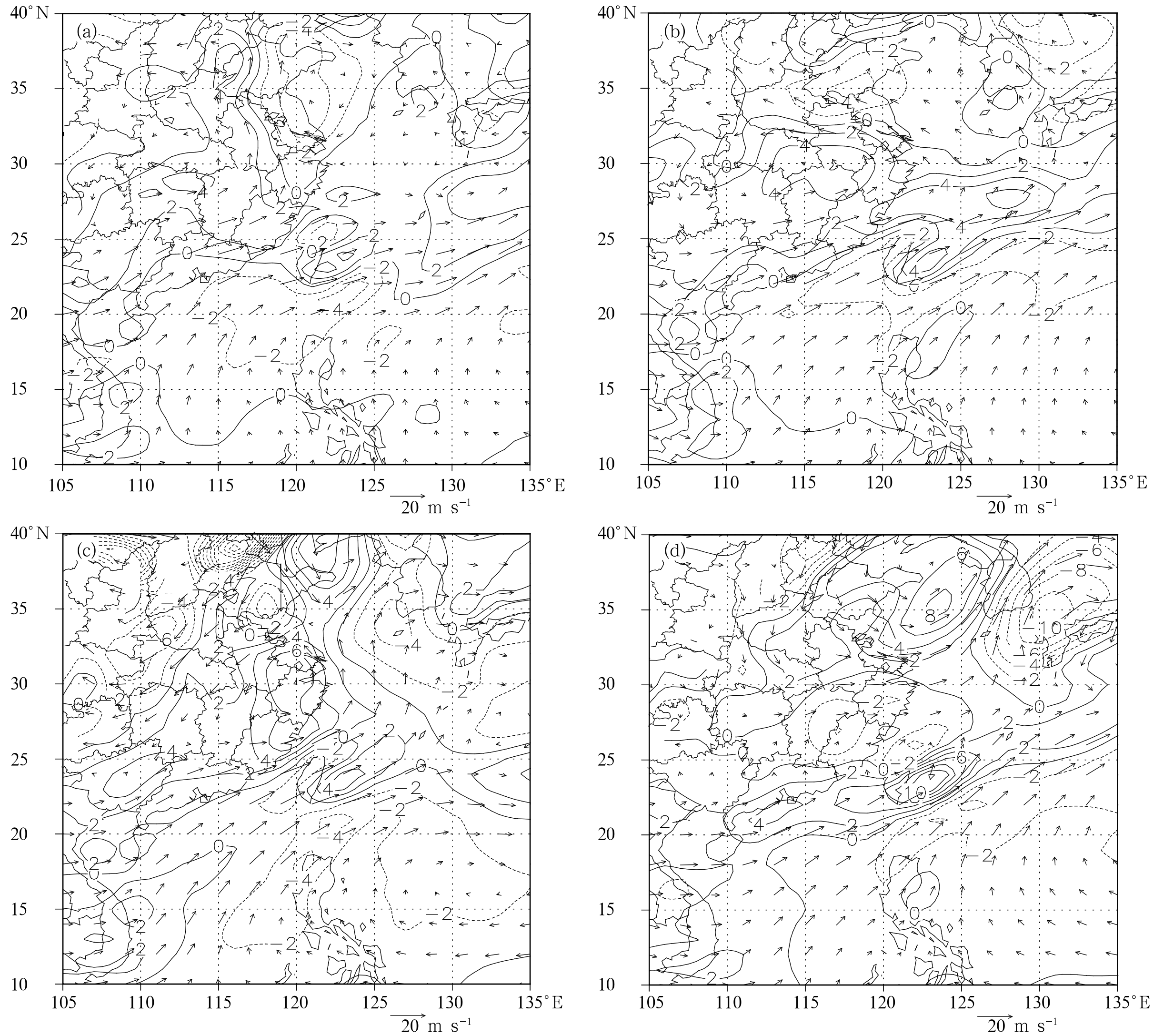

Fig.5. EPV-inversed balanced winds (vector; m s^{-1}) and its relative vorticity (solid line; 10^{-5} s^{-1}) at 850 hPa during the periods of Meiyu front's formation and development at (a) 2000 BT 3, (b) 0800 BT 5, (c) 1400 BT 7, and (d) 0800 BT 10 June 2006.

extent though it is non-divergence flow. Therefore, the evolution of nonlinear balanced flow plays an important role in the formation, development, and movement of the Meiyu front.

4.4 The evolution of the unbalanced flow

Supposed that the real wind V can be separated into two parts of rotational (V_ψ, calculated from stream function) and divergence winds (V_Φ, calculated from potential function), i.e., $V = V_\psi + V_\Phi$. After the balanced winds (non-divergence wind) are obtained from EPV inversion, the unbalanced winds (non-rotational winds) can be calculated out after real winds minus balanced winds.

Figure 6 presents the 850-hPa unbalanced winds (non-rotational winds) and its divergence in the different developing stages of Meiyu front. In Stage I, there are two convergence centers on the Meiyu front, which are consistent with its rainfall centers (Fig.6a). The formation of the two convergence centers are related to three unbalanced flows: an east flow in the bottom of high pressure system located in the Korean Peninsula and the east of North China, a north flow from the east of North China, and a south flow in the south

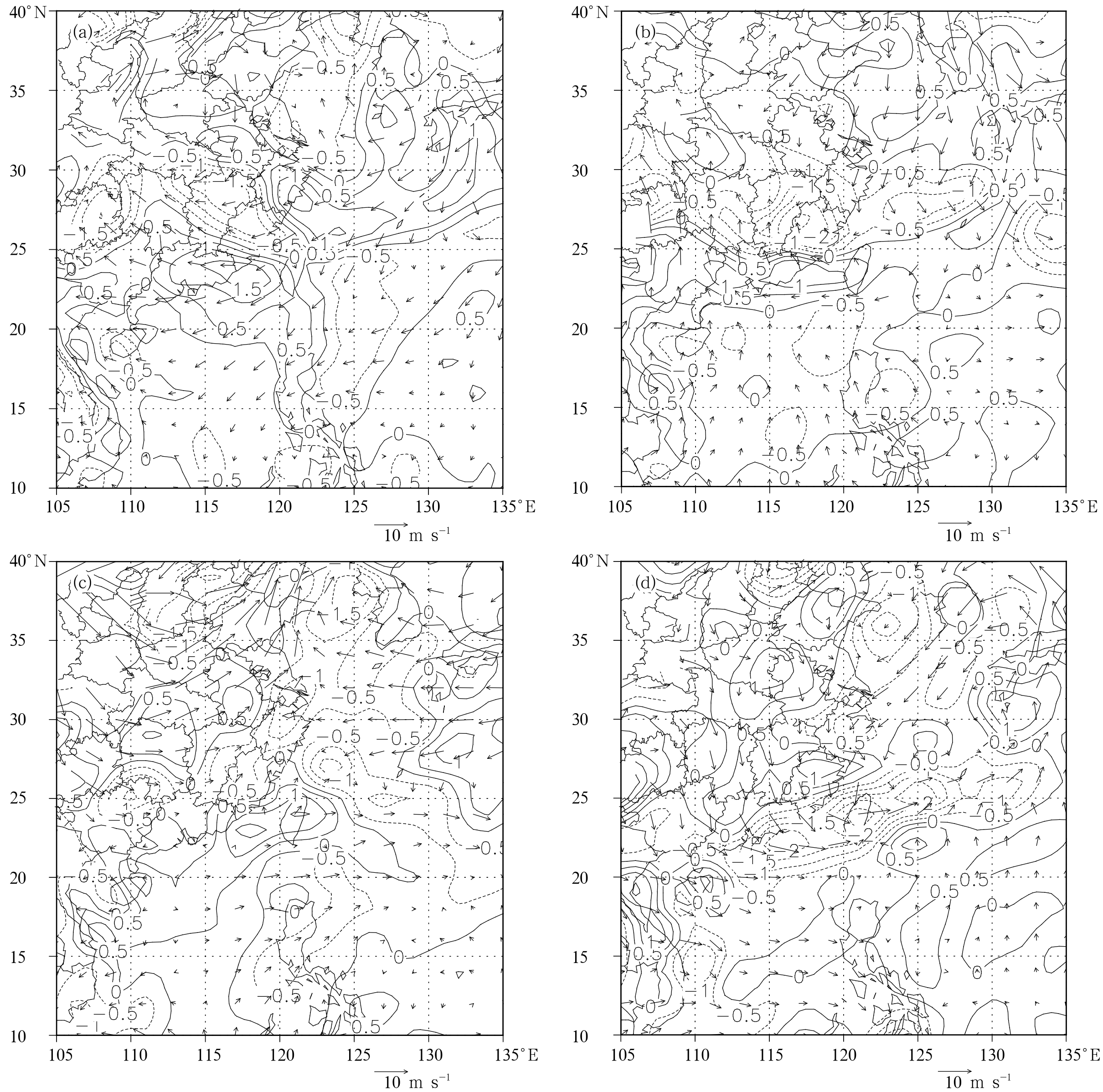

Fig.6. EPV-inversed unbalanced winds (vector; m s^{-1}) and its divergence (solid line; 10^{-5} s^{-1}) at 850 hPa during the periods of Meiyu front's formation and development at (a) 2000 BT 3, (b) 0800 BT 5, (c) 1400 BT 7, and (d) 0800 BT 10 June 2006.

of Meiyu front. The former two come from the high pressure band in the north of Meiyu front. In Stage II, a quasi-WE oriented convergence band always maintains on the Meiyu front, whose formation is mainly associated with the north divergence winds from the east of North China high and the south divergence winds in the south of Meiyu front, i.e., the two important divergence flows are still related to the high pressure system in the two sides of Meiyu front (Fig.6b). In Stage III, the divergence flows forming the Meiyu front convergence band are northwest winds from the rear of deep North China low trough and west winds in the bottom of the trough (Fig.6c). At 0800 BT 10 June, the Meiyu front totally propagated southward to the sea along with the convergence band. At this time, the main divergence flows forming the convergence band were north flows from the mid-latitudes (Fig.6d).

Therefore, the unbalanced flows forming the Meiyu front convergence band are still relevant to the high pressure systems in the two sides of Meiyu front, especially the high pressure system in its north side and the activity of the low trough. In the formation and stably maintaining stage, the unbalanced flow (north flow) from the North China high was the main contributor to the Meiyu front convergence band. In the fast southward shifting stage, the unbalanced flow from the North China low trough is the main factor of the convergence band. Nevertheless, compared with the balanced flow, the evolution of unbalanced flow is not continuous, and therefore hard to predict.

5. Piecewise PV inversion of Meiyu frontal heavy rain system

5.1 *The separation of the piecewise EPV*

According to the studying, the PV perturbation can be separated into different parts to explore the effects of different PV perturbations. Davis and Emanuel (1991) divided the PV perturbation of 1000–100 hPa into the lower boundary potential temperature (the interpolation of 1000 and 900 hPa), PV perturbations in the mid-lower troposphere (850–500 hPa), and the upper level (400–100 hPa). Chen et al. (2003) further separated the mid-lower PV perturbations into two parts associated or unassociated with condensation release heating in his studying on the Meiyu front with PV inversion method. The data used in their study are taken at 10 levels, without the boundary layer. Here, with every 6-h 21 levels NCEP data, the boundary layer can be included in the research. On the basis of the above researches, the PV perturbations are divided into the following parts: 1) the lower boundary potential temperature perturbations (θ', the interpolation of 1000 and 975 hPa), 2) the boundary layer (the lower troposphere) PV perturbations (the PV perturbations at 975–900 hPa), 3) the PV perturbations associated with latent heat release (LHR; the PV perturbations of relative humidity greater than or equal to 70% at 850–500 hPa), 4) the PV perturbations not associated with LHR (the PV perturbations of relative humidity less than 70% at 850–500 hPa), and 5) the upper-level PV perturbations (the PV perturbations at 450–150 hPa), to analyze the different roles of lower boundary potential temperature, the boundary layer physics, the diabatic heating, dry air dynamics in the mid-lower troposphere, and upper-level PV perturbations in the Meiyu front. The separation of PV perturbations is based on the assumption that, the lower boundary θ' is related to surface physical like heating, the generation of boundary layer PV perturbations is associated with the physical between surface and boundary layer such as latent and sensible heat exchange and friction etc., the diabatic heating resulting from LHR in the mid-lower troposphere makes positive PV of moist atmosphere, and PV perturbation in the upper level has a certain effect on the atmosphere in the lower troposphere.

5.2 *The effects of lower boundary potential temperature anomalies*

Bretherton (1966) pointed out that, the positive θ' has an effect equivalent to positive PV anomaly (perturbation), and vice versa. The negative θ' (cold air) is reflected as a trough on its above levels through hydrostatic balance, which resists the effects of θ'. Holopainen and Kaurola (1991) discussed that the resistance of lower boundary θ' and its above PV perturbations takes place in a shallow layer. What are the effects of lower boundary θ' on the Meiyu frontal heavy rain system? Figure 7 gives the 850-hPa balanced winds and its relative vorticity by the inversion of lower boundary θ' in different developing stages of Meiyu front. In Stage I, the lower boundary θ' is not beneficial to the formation of Meiyu front, with a strongest negative vorticity of -0.8×10^{-5} s^{-1}. In Stage II, the lower boundary θ' is not conducive to the maintaining of Meiyu front, with the vorticity band of its balanced winds and Meiyu front both in a WE orientation, and a strongest negative vorticity of -1.2×10^{-5} s^{-1}. In Stage III, the role of the lower boundary θ' is still negative and not favorable to the development of Meiyu front, with a strongest negative vorticity of -0.6×10^{-5} s^{-1}. In Stage IV, the vorticity band of its balanced winds and the Meiyu front are also both in an NE-SW direction. It can be concluded that the lower boundary θ' seems to be always not

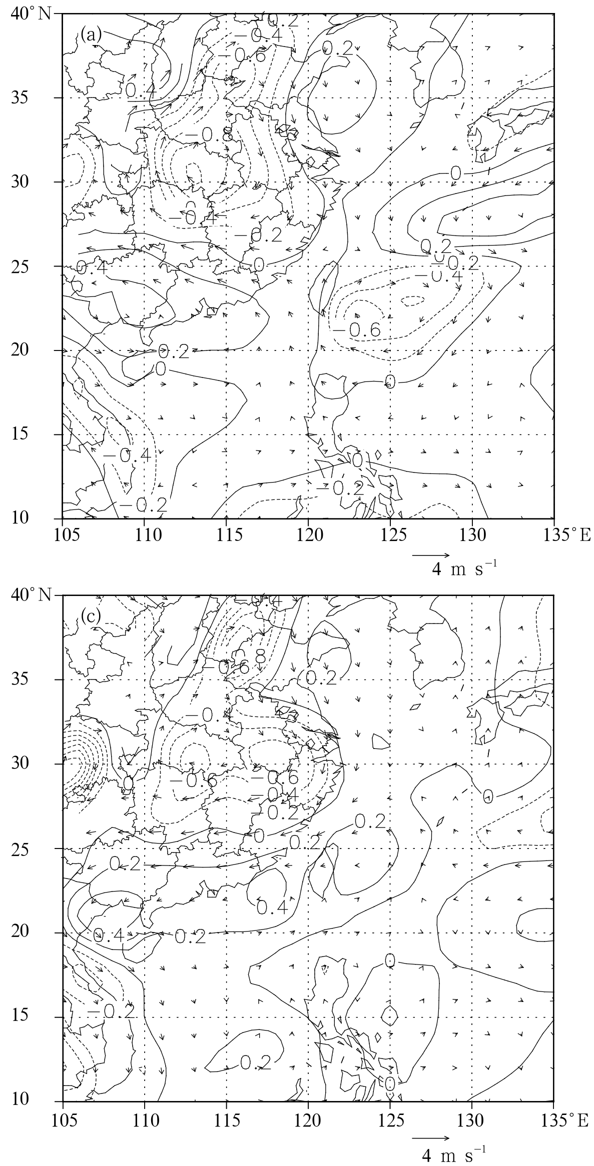

Fig.7. EPV-inversed balanced winds (vector; m s^{-1}) and its relative vorticity (solid line; 10^{-5} s^{-1}) at 850 hPa induced from lower boundary potential temperature perturbation during the periods of Meiyu front's formation and development at (a) 2000 BT 3, (b) 0800 BT 5, (c) 0200 BT 7, and (d) 0800 BT 10 June 2006.

advantageous to the formation, maintenance, and development of the Meiyu front.

Why is the lower boundary θ' not beneficial to the formation, maintenance, and development of the Meiyu front? After the analysis of surface θ' in detail, the temperature near the Meiyu front is lower than that in the two sides of Meiyu front. This is mainly due to the temperature decrease by the rainfall evaporation on the Meiyu front and the barrier of the Meiyu frontal clouds to solar short-wave radiation. There is a negative θ' band along the Meiyu front. There exist obvious diurnal variations because the surface θ' is largely influenced by solar radiation. The variation is more obvious especially in the sparse cloud area to the north of Meiyu front, with the largest daily range between 1400 and 0200 BT (as to every 6-h analysis). The surface temperature perturbations are even opposite, and therefore the induced balanced wind circulation is opposite correspondingly. Figure 8 depicts 850-hPa balanced winds and relative vorticity induced

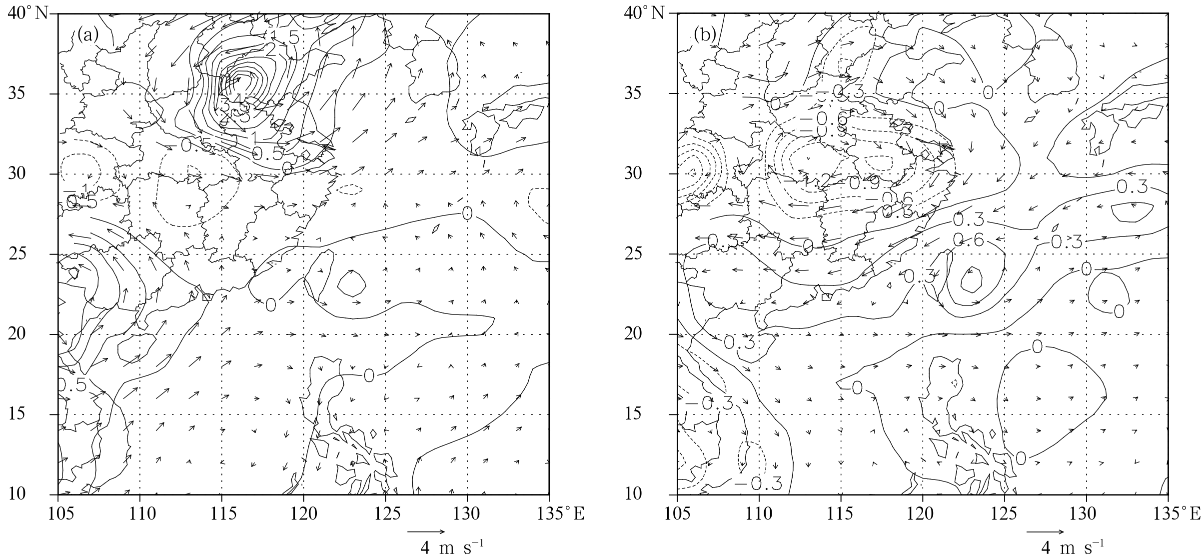

Fig.8. As in Fig.7, but for (a) 1400 BT 5 and (b) 0200 BT 6 June 2006.

from the lower boundary θ' at 1400 BT 5 and 0200 BT 6 June, respectively. The variable θ' is positive in North China at 1400 BT 5 June (afternoon), with an induced cyclonic vortex and a positive vorticity of 4×10^{-5} s^{-1}. It can be seen that the lower boundary θ' has an obvious effect on heavy rain system of the Meiyu front. While the lower boundary θ' on the Meiyu front is negative and therefore has a negative contribution to the Meiyu front. At 0200 BT 6 June (midnight), an anti-cyclonic circulation is induced in the negative θ' area to the north of Meiyu front, with a negative vorticity of -1.2×10^{-5} s^{-1}. The vorticity on the Meiyu front is also negative.

5.3 *The effects of low level (boundary layer) PV perturbations*

Not neglected is the role of boundary layer physics in the development of heavy rain systems. Sang(1997) indicated that the atmospheric boundary layer physics played a very important role in the momentum, heat, and moisture vertical transportation. Zhai et al. (2003) revealed that the small disturbances on the mesoscale convergence line in the boundary layer had a role in the triggering of the rainstorms. The boundary layer physical processes are mainly the latent and sensible heat exchange between the surface and boundary layer atmosphere, and the effects of surface friction on the boundary layer air. The generation of PV in the boundary layer is mainly associated with the physics in the boundary layer. What are the effects of PV anomalies in the boundary layer? Figure 9 gives the 850-hPa balanced winds and relative vorticity induced from lower-level PV anomalies in the different developing stages of Meiyu front. In Stage I, a weak cyclonic circulation forms in the north of Hunan Province and the south of Hubei Province, where there is a Meiyu frontal rain band. A positive vorticity center is corresponded with the weak circulation, with a vorticity of 0.6×10^{-5} s^{-1}. In Stage II, the induced vorticity band is in a quasi-WE orientation. The positive vorticity center on the band moves eastward to the north of Fujian Province and the south of Zhejiang Province, with a positive vorticity of 0.3×10^{-5} s^{-1}. And the heavy rainfall also moves to this area. This indicates that the PV perturbation in the boundary layer is closely related to the Meiyu frontal heavy rain system. In Stage IV, the positive vorticity band moves to the south, with a maximum vorticity of 1×10^{-5} s^{-1}. The effects of lower-level PV anomalies on the Meiyu front are the strongest. At the same time, a strong NE-SW oriented positive vorticity band is in the east of North China, which is related to the North China low trough, with a maximum vorticity of 2.5×10^{-5} s^{-1}.

Viewed from the relative vorticity of balanced

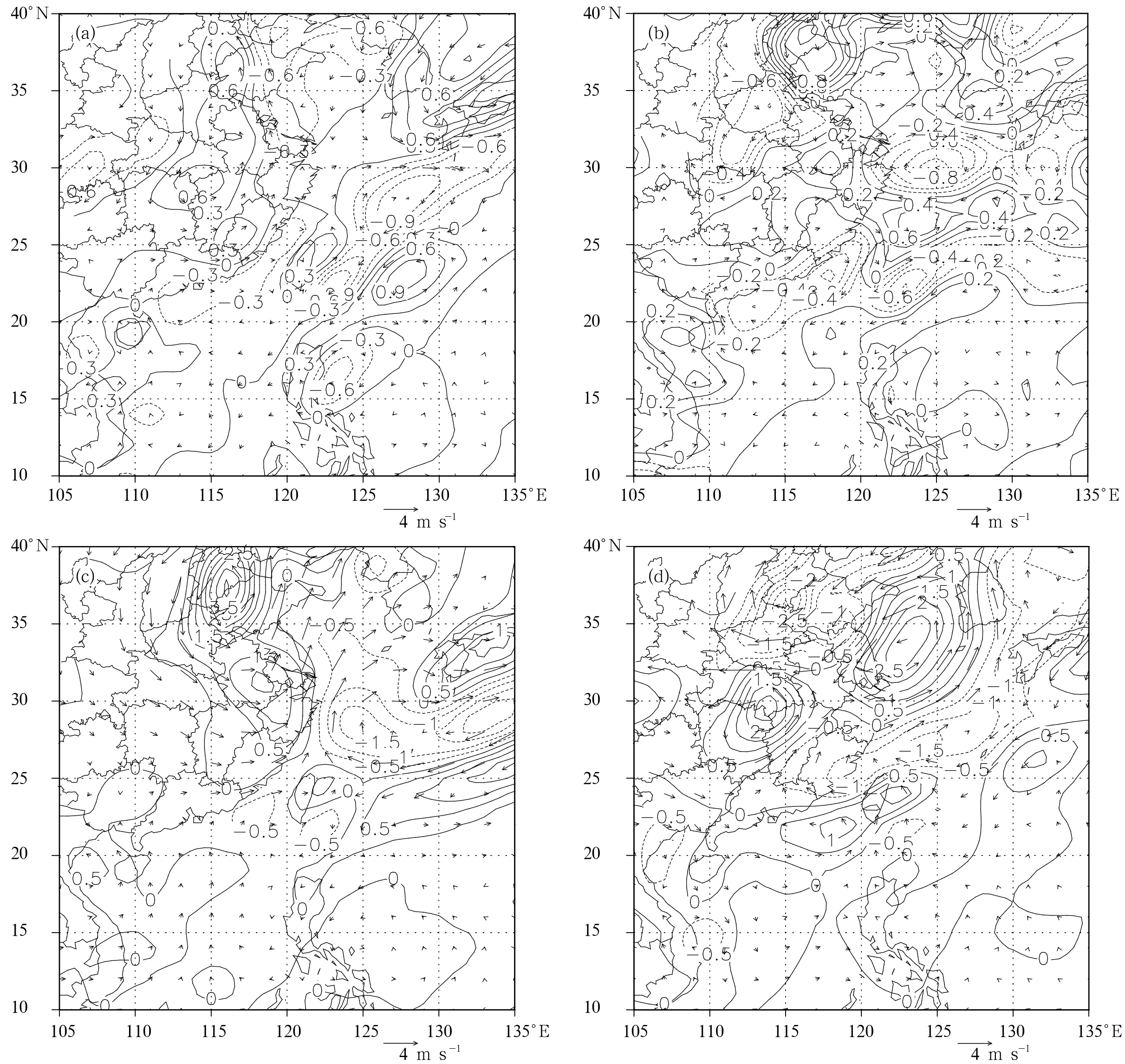

Fig.9. As in Fig.7, but inversed from potential vorticity perturbation in the lower troposphere (950–900 hPa) during the periods of Meiyu front's formation and development.

winds induced from low-level PV perturbation, it plays an important role in the maintenance and development of Meiyu front, varying with the evolution of Meiyu frontal weather system. This indicates that the generated PV perturbation by physical processes in the boundary layer exerts an influence on the formation, maintenance, and development of the Meiyu front. Therefore, the effects of the boundary layer on the Meiyu frontal heavy rain system are needed further investigation.

5.4 *The effects of mid-lower PV anomalies*

5.4.1 The effects of positive mid-lower PV anomalies associated with diabatic heating

There have been a lot of researches and documentations about the effects of diabatic heating like LHR on the heavy rain system and their interaction. Durran and Klemp (1982) thought that the LHR reduced the hydrostatic instability of the atmosphere. Hoskins et al. (1985) further pointed out that the penetration

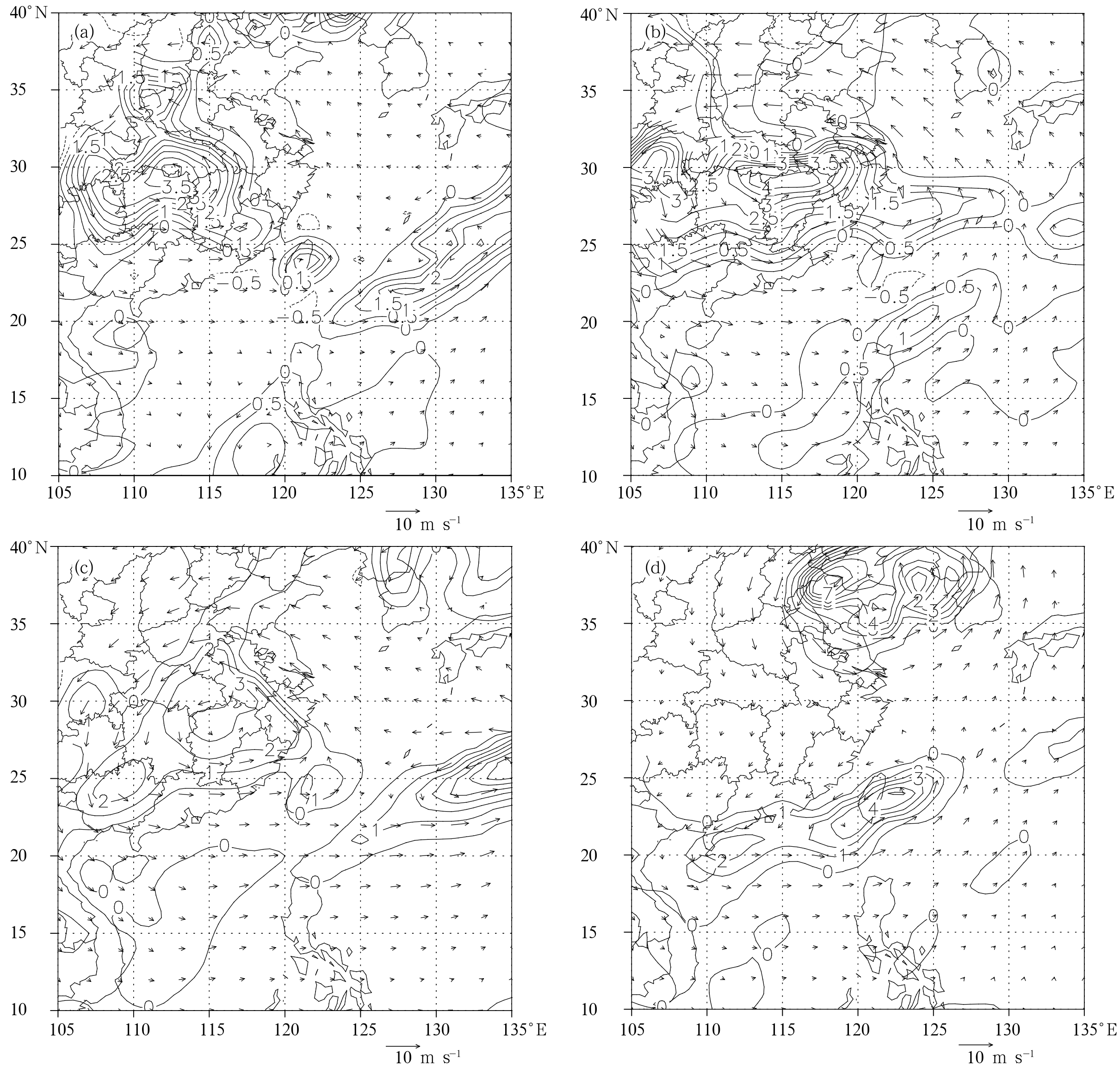

Fig.10. As in Fig.7, but inversed from potential vorticity perturbation related to diabatic heating in the middle-lower troposphere (850–500 hPa).

capability of circulation related to lower and upper boundary PV anomalies was enhanced and therefore the interaction between the vortices after the hydrostatic instability of the atmosphere reduced. Chen et al. (2003) claimed that the LHR of Meiyu front rainfall had an important role in the intensification and frontogenesis of the Meiyu front. The numerical simulations (Michael and Lackmann, 2005; Wang and Xiao, 1997) also proved the importance of LHR (cumulus convection) in the LLJ formation. Hence, the LHR is important to the development and formation of rainfall synoptic systems. Here, the PV perturbation relevant to the LHR is inversed to investigate the role played by diabatic heating in the formation, maintenance, and development of Meiyu front.

Figure 10 depicts the 850-hPa balanced winds and relative vorticity induced from the positive PV anomalies related to the LHR in the different developing stages of Meiyu front. In Stage I, a cyclonic circulation induced from positive PV anomalies related to the LHR forms in the west part of Meiyu front (from the north of Hunan to the north of Jiangxi), with a positive vorticity of 4×10^{-5} s^{-1}, which is equivalent to the vorticity calculated by real winds. The rainfall on the Meiyu front also takes place there. When the Meiyu frontal rainfall shifting to the east, the induced balanced winds form a WE-oriented vorticity band and the maximum vorticity center also moves to the east, with a maximum vorticity of 4×10^{-5} s^{-1}. The maximum positive vorticity on the band is in consistence with the heavy rain area. This also implies that the LHR has an important role in the generation of mid-lower PV perturbation which will exert a feedback on the Meiyu frontal heavy rain system. In Stage III, the balanced winds induced from PV anomalies relevant to LHR also form an NE-SW positive vorticity band, with the maximum vorticity center matching with the heavy rain center on the Meiyu front. In Stage IV, the NE-SW oriented positive vorticity band induced by balanced winds also move to the sea, with the positive vorticity band corresponding with the Meiyu frontal rain band.

It can be seen that the PV perturbation associated with LHR plays a significant role in the formation, maintenance, and development of Meiyu front. Its positive vorticity band induced from balanced winds is in accordance with the Meiyu front, with the vorticity equivalent to that calculated from real winds and the maximum positive vorticity band is in accordance with the Meiyu frontal heavy rain center. Therefore, the diabatic physical process of LHR is an important mechanism for the development of heavy rain system on the Meiyu front.

5.4.2 The effects of the rest mid-lower PV anomalies

Figure 11 shows the 850-hPa balanced winds and relative vorticity induced from other PV anomalies unrelated to the LHR in the different developing stages of Meiyu front. In Stage I, a cyclonic circulation is in the north of Henan Province and to the north of Meiyu front, with a maximum vorticity of 6×10^{-5} s^{-1} (Fig.11a). It is beneficial to the formation of Meiyu front. In Stage II, a cyclonic circulation forms in the east of Hubei Province, which is a little away from and in the north of Meiyu front and favorable to the Meiyu frontal maintenance, with a maximum vorticity of 6×10^{-5} s^{-1} (Fig.11b). In Stage III, a cyclonic circulation is in the east of Hubei Province and the north of Henan Province, with a maximum vorticity of 5×10^{-5} s^{-1} (Fig.11c). The southwest flow at the bottom of the circulation is conducive to the maintenance and development of the Meiyu front. In Stage IV, a strong anti-cyclonic circulation occurs in the north of Fujian Province. It is found with detailed analysis that the circulation forms at 0800 BT 8 June, when the rainfall in the north of Fujian is over. After that, the anti-cyclonic circulation moves southeastward and pushes the Meiyu front to the sea. Hence, the anti-cyclonic circulation plays an important role in the Meiyu front shifting southeastward.

5.5 *The effects of the upper-level PV anomalies*

Hoskins et al. (1985) pointed out that the positive PV disturbance in the stratosphere can penetrate into the troposphere and induce a cyclonic circulation in the mid-troposphere, which even can penetrate through the whole troposphere to the surface. Young and Browning (1987) also found that the dry intrusion from mid-latitudes has a high PV tongue, which can extend from the stratosphere with copious PV to the lower latitudes. During its mature period, it is observed that the PV tongue of the stratosphere can further develop and generate cyclonic circulation and forms a large-scale vortex (1000–2000 km) near the surface. However, Chen et al. (2003) pointed out that the PV in the upper troposphere contributed negatively to the Meiyu front. Then, what is the role played by the upper-level PV disturbance in this Meiyu front? Figure 12 shows the 850-hPa balanced winds and its relative vorticity induced from the upper-level PV anomalies in the different developing stages of Meiyu front. In Stage I, the upper-level PV perturbation exerts less effects on the Meiyu front. The vorticity of balanced winds is negative in the north of Fujian Province and northwest of Jiangxi Province, with a strongest negative vorticity of -0.06×10^{-5} s^{-1},

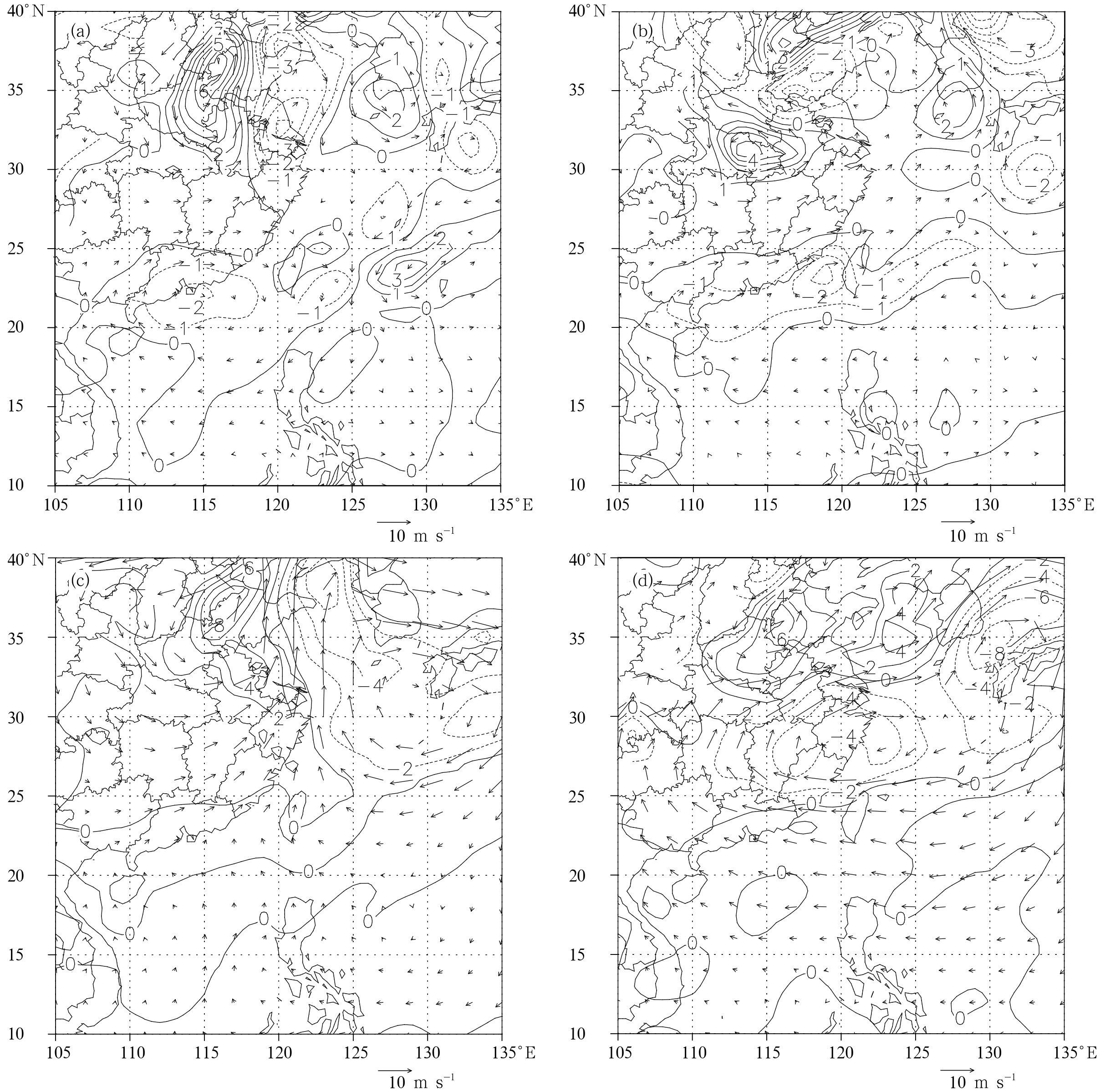

Fig.11. As in Fig.7, but inversed from the rest potential vorticity perturbation unrelated to diabatic heating in the middle-lower troposphere (850–500 hPa).

and positive in the north of Hunan Province, with a maximum vorticity of 0.02×10^{-5} s^{-1} (Fig.12a). In Stage II, the vorticity of balanced winds is negative in the heavy rain area of the Meiyu front (in the north of Fujian Province and the south of Zhejiang Province), with a strongest negative vorticty of -0.03×10^{-5} s^{-1}. In Stage III, the upper-level PV disturbance makes a negative contribution to the Meiyu front, especially to the heavy rain area in the north of Fujian Province, with a strongest negative vorticity of -0.04×10^{-5} s^{-1}. But in the disappearing period of Meiyu frontal rain band in land, the deep north trough develops and the upper-level PV disturbance induces a cyclonic vortex at 850 hPa, its center in the Changjiang-Huaihe River basin, with a maximum vorticity of 1.5×10^{-5} s^{-1}. At this time, the vortex is in the north of Meiyu front and the maximum vorticity on the Meiyu front is 0.2×10^{-5} s^{-1}.

On the whole, the upper-level PV disturbance exerts a negative effect on the Meiyu front, especially in the heavy rain area, in the formation, development, maintenance, and fast southward shifting of the Meiyu front. But the role is much weaker than other PV perturbations. In Stage IV, due to the development, eastward movement, and southward shifting of North China low trough, the upper-level PV disturbance induces a cyclonic votex in the north of Meiyu front and makes a positive contribution to the development and maintenance of Meiyu front. But it is not advantageous to the Meiyu front maintaining locally. On the contrary, the northwest winds in the rear of deep low trough push the Meiyu front southward to the sea. Therefore, the role played by the upper-level PV disturbances in the Meiyu front is different in the different stages of the Meiyu front.

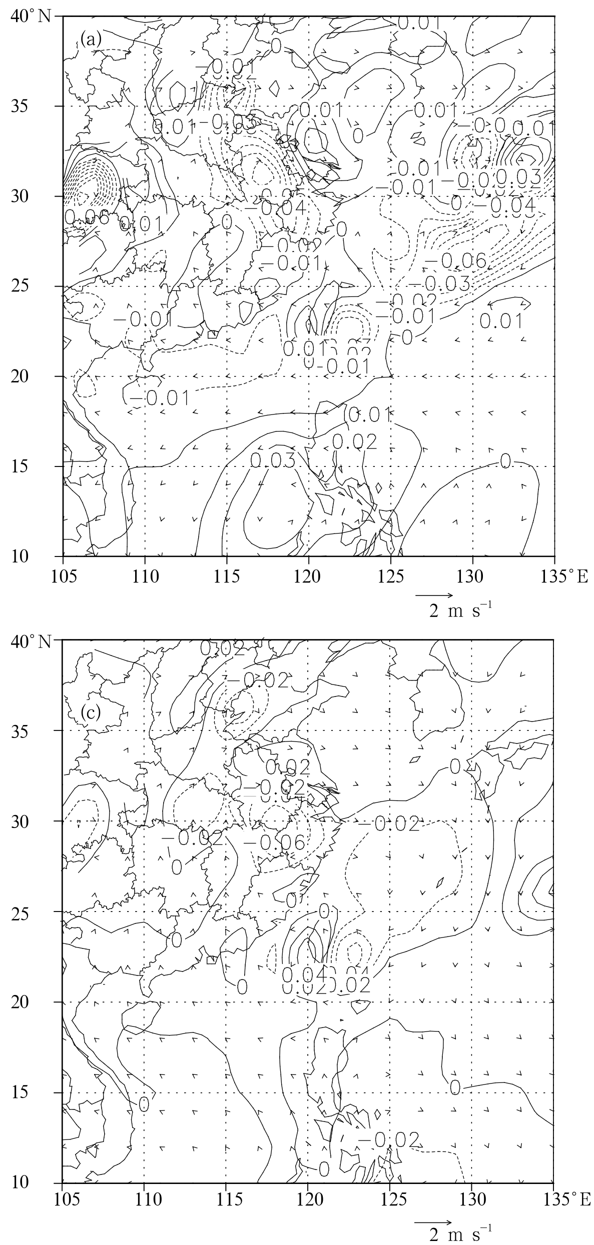

Fig.12. As in Fig.7, but inversed from potential vorticity perturbation in the upper level (450–100 hPa) of the troposphere.

6. Conclusions and discussions

In this study, a Meiyu front process inducing continuous heavy rain in the north of Fujian Province is analyzed in detail to investigate the atmospheric characteristics and the main synoptic system in the different stages of the Meiyu front evolution. At the same time, the PV perturbations associated with different physics are separated with PV inversion method to explore the role of different physics in the formation, development, and maintenance of Meiyu front. The results are as follows:

(1) The main weather pattern in the formation and development of Meiyu front is that two main important high pressure systems are in the mid-lower troposphere of 850 hPa, i.e., the West Pacific subtropical high and North China high, with the Meiyu front in the lower pressure band between the south and north high pressure systems. The westerly flow is flat in the mid-latitudes of 500 hPa and short waves in the west flow form and move eastward to influence Meiyu frontal rainfall. The upper-level jet stream at 200 hPa is located in the north of 30°N and there are several jet cores forming on the jet axis and moving eastward, with heavy rain on the Meiyu front in the right of the jet stream entrance. The South Asian high is maintaining stably at 100 hPa, within 27°–28°N and the Meiyu front in the divergence flow of upper-level northwest and northeast winds.

(2) There is a close relationship between the Meiyu front and the PV in the lower troposphere of 850 hPa. The PV can denote Meiyu front. The positive PV disturbance on the Meiyu front matches with the heavy rain area. It may be related to the LHR associated with Meiyu frontal rainfall condensation, i.e., the diabatic heating may generate the PV on the Meiyu front band in the lower troposphere.

(3) The EPV inversed balanced flow satisfying the nonlinear balanced equation represents the real flow to a large extent, and therefore it is the main component of real winds. The variation of nonlinear balanced flow is of importance to the formation, development, and movement of the Meiyu front. The unbalanced flow of Meiyu frontal convergence band is mainly related to the high pressure system in the two sides of Meiyu front, especially to the activities of high pressure system and low trough in its north side, i.e., the unbalanced flow (north flow) from North China high is the main confluent flow of the Meiyu frontal convergence band in the period of Meiyu front maintaining stage, while the unbalanced flow from North China low trough is the main factor of the convergence band in the period of the Meiyu front fast shifting southward.

(4) The diagnosis of the different PV perturbations shows that, the low-level PV perturbation exerts some influence on the formation, development, and maintenance of the Meiyu front. But the role may be different in the different stages of Meiyu front. Hence it should be paid attention to the role of generated PV disturbance by the boundary layer physics in the maintenance and development of the Meiyu front. On the whole, the upper-level PV perturbation is not beneficial to the formation, development, and maintenance of Meiyu front. Especially in the heavy rain area on the Meiyu front, its effect is relatively weak compared with other PV disturbance. But in the stage of North China low trough shifting southward, the effect of upper-level PV perturbation is enhanced obviously. The lower boundary θ' is not advantageous to the formation, maintenance, and development of the Meiyu front. This is resulting from the relative lower surface temperature due to the rainfall evaporation on the Meiyu front and the barrier of Meiyu frontal clouds to the solar radiation. The surface temperature is of large daily range because it is influenced largely by the solar radiation and therefore may exert different effects on the Meiyu frontal heavy rain systems.

(5) The positive PV perturbation associated with LHR is one of the main factors influencing the Meiyu front formation, maintenance, and development. Its vorticity of balanced winds is near to that calculated from real winds on the Meiyu front, with the maximum vorticity center in accordance with the heavy rain area on the Meiyu front. Hence, the diabatic physics related to rainfall condensation heat is one of the main mechanisms responsible for the formation, development, and maintenance of the Meiyu front. The other PV disturbance unrelevant to the LHR also has a

certain effect on the Meiyu front. In the late stage of the Meiyu front, the induced anti-cyclonic circulation exerts some influence on the Meiyu front's southeastward movement.

Here performed is only a case study of continuous heavy rain process with PV inversion. As to Meiyu frontal heavy rain processes on different synoptic situations, the role played by different PV disturbances in the formation, development, and maintenance of the Meiyu frontal heavy rain systems may be different. Therefore, typical continuous heavy rain processes on the Meiyu front are needed to make further diagnostic analysis with PV inversion method, conclude the physical image of PV distribution and evolution of Meiyu frontal heavy rain processes, deepen the knowledge of Meiyu frontal heavy rain, and provide a clue for heavy rain forecast. Besides, the diagnostic study of this case implies that the PV perturbations related to boundary layer physics and LHR are the main factors influencing the development of Meiyu frontal heavy rain system. Hence, the analysis is needed to deepen into the role of boundary layer physics, and diabatic physics and numerical sensitivity experiment should be carried out to further reveal the role of PV perturbation in the Meiyu frontal development.

Acknowledgement. The author is very grateful to the help of Prof. Da-lin Zhang from Maryland University of the United States for generously providing a FORTRAN program code of potential vorticity inversion.

REFERENCES

Bretherton, F. P., 1966: Critical layer instability in baroclinic flows. *Quart. J. Roy. Meteor. Soc.*, **92**, 325–334.

Charney, J. G., 1962: Integration of the primitive and balance equations. Proc. Symp. on Numerical Weather Prediction, Tokyo, Japan, WMO/IUGG, 131–152.

Chen George Tai-Jen, Wang Chung-Chieh, and Liu Stefano Chih-Shin, 2003: Potential vorticity diagnostics of a Meiyu front case. *Mon. Wea. Rev.*, **131**, 2680–2696.

Chen, G. T. J., and C. P. Chang, 1980: The structure and vorticity budget of an early summer monsoon trough (Mei-Yu) over southeastern China and Japan. *Mon. Wea. Rev.*, **108**, 942–953.

Chen Lifang and Gao Kun, 2006: The simulation of the uneven characteristics of Meiyu frontal structure. *Acta Meteor. Sinica*, **64**(2), 164–179. (in Chinese)

Cho, H. R., and G. T. J. Chen, 1995: Mei-Yu frontogenesis. *J. Atmos. Sci.*, **52**, 2109–2120.

Davis, C. A., 1992: Piecewise potential vorticity inversion. *J. Atmos. Sci.*, **49**, 1397–1411.

Davis, C. A., and K. A. Emanuel, 1991: Potential vorticity diagnosis of cyclogenesis. *Mon. Wea. Rev.*, **119**, 1929–1953.

Demirtas, M., and A. J. Thorpe, 1999: Sensitivity of short-range weather forecasts to local potential vorticity modifications. *Mon. Wea. Rev.*, **127**, 922–939.

Durran, D. R., and J. B. Klemp, 1982: On the effects of moisture on the Brunt-V frequency. *J. Atmos. Sci.*, **39**, 2152–2158.

Hakim, G. J., D. Keyser, and L. F. Bosart, 1996: The Ohio valley wave-merger cyclogenesis event of 25–26 January 1978. Part II: Diagnosis using quasi-geostrophic potential vorticity inversion. *Mon. Wea. Rev.*, **124**, 2176–2205.

Holopainen, E., and J. Kaurola, 1991: Decomposing the atmosphere flow using potential vorticity framework. *J. Atmos. Sci.*, **48**, 2614–2625.

Hoskins, B. J., M. E. McIntyre, and A. W. Robertson, 1985: On the use and significance of isentropic potential vorticity maps. *Quart. J. Roy. Meteor. Soc.*, **111**, 877–946.

Huo Zonghui, Zhang Da-Lin, and J. R. Gyakum, 1998: An application of potential vorticity inversion to improving the numerical prediction of the March 1993 superstorm. *Mon. Wea. Rev.*, **126**, 424–436.

Huo Zonghui, Zhang Da-lin, and J. R. Gyakum, 1999: Interaction of potential vorticity anomalies in extratropical cyclogenesis. Part II: Sensitivity to initial perturbation. *Mon. Wea. Rev.*, **127**, 2563–2575.

Jiang Xiaoyan and Ni Yunqi, 2005: Numerical simulation study on the evolution mechanism of meso-β scale convective system along the Meiyu front. *Acta Meteor. Sinica*, **63**(1), 77–92. (in Chinese)

Kato, K., and J. E. Martin, 1985: On the abrupt change in the structure of the Baiu front over the China continent in late May of 1979. *J. Meteor. Soc. Japan*, **63**, 20–35.

Liu Junjie, Ding Yihui, and He Jinhai, 2003: The structure analysis of a typical Meiyu front. *Acta Meteor. Sinica*, **61**(3), 291–303. (in Chinese)

Michael, J. B., and G. M. Lackmann, 2005: The influence of incipient latent heat release on the precipitation distribution of the 24–25 January 2000 U.S. east coast cyclone. *Mon. Wea. Rev.*, **133**, 1913–1937.

Sang Jianguo, 1997: The vortex structure in convective boundary layer. *Acta Meteor. Sinica*, **55**(3), 285–296.

Wang Jianjie and Guo Xiaorong, 1997: Numerical simulation of the earliest torrential rain event over South China in 1996. *J. Appl. Meteor.*, **8**(3), 257–266. (in Chinese)

Wang Jianjie and Li Zechun, 2002: Numerical simulation and diagnostic analysis on mesoscale convective systems of a torrential rain case in Meiyu period of 1998. *Acta Meteor. Sinica*, **60**(2), 146–156. (in Chinese)

Wang Zhi, Zhai Guoqing, and Gao Kun, 2003: A numerical simulation of a mesoscale low vortex in the middle valleys of Yangtze River. *Acta Meteor. Sinica*, **61**(1), 66–77. (in Chinese)

Wu Chun-Chieh, Huang Treng-Shi, and Chou Kun-Hsuan, 2004: Potential vorticity diagnosis of the key factors affecting the motion of typhoon Sinlaku (2002). *Mon. Wea. Rev.*, **132**, 2084–2093.

Wu Rongsheng, Gao Shouting, Tan Zhemin, et al., 2004: *Meiyu Frontogenesis and Mesoscale Disturbances*. China Meteorological Press, Beijing, 168 pp. (in Chinese)

Young, M. V., and G. A. Browning, 1987: Interpretation of satellite imagery of a rapidly developing cyclone. *Quart. J. Roy. Meteor. Soc.*, **113**, 1089–1115.

Zhai Guoqin, Wang Zhi, and He Bin, 2003: Formation and evolution analysis of the mesoscale vortex group in the middle and lower reaches during Meiyu of the Yangtze River. *Acta Meteor. Sinica*, **61**(6), 661–672.

Zhao Sixiong, Tao Zuyu, Sun Jianhua, et al., 2004: *Study on the Mechanism of the Formation and Development of Heavy Rainfall on the Meiyu Front in the Yangtze River*. China Meteorological Press, Beijing, 281 pp. (in Chinese)

Zhou Yi, Kou Zheng, and Wang Yunfeng, 1998: Potential vorticity inversion diagnosis about the importance of latent heat in the cyclone rapid development process. *Meteor. Sci.*, **18**(4), 355–360. (in Chinese)